JACS
JOURNAL OF THE AMERICAN CHEMICAL SOCIETY

Communication

pubs.acs.org/JACS

^{129}Xe NMR Relaxation-Based Macromolecular Sensing

Muller D. Gomes,[†,‡] Phuong Dao,[†,‡] Keunhong Jeong,[†,‡] Clancy C. Slack,[†,‡] Christophoros C. Vassiliou,[‡] Joel A. Finbloom,[‡] Matthew B. Francis,[†,‡] David E. Wemmer,[‡,§] and Alexander Pines*[,†,‡]

[†]Materials Sciences Division, Lawrence Berkeley National Laboratory, Berkeley, California 94720, United States
[‡]Department of Chemistry, University of California, Berkeley, California 94720, United States
[§]Physical Biosciences Division, Lawrence Berkeley National Laboratory, Berkeley, California 94720, United States

Supporting Information

ABSTRACT: We report a ^{129}Xe NMR relaxation-based sensing approach that exploits changes in the bulk xenon relaxation rate induced by slowed tumbling of a cryptophane-based sensor upon target binding. The amplification afforded by detection of the bulk dissolved xenon allows sensitive detection of targets. The sensor comprises a xenon-binding cryptophane cage, a target interaction element, and a metal chelating agent. Xenon associated with the target-bound cryptophane cage is rapidly relaxed and then detected after exchange with the bulk. Here we show that large macromolecular targets increase the rotational correlation time of xenon, increasing its relaxation rate. Upon binding of a biotin-containing sensor to avidin at 1.5 μM concentration, the free xenon T_2 is reduced by a factor of 4.

Very strong NMR signals from hyperpolarized ^{129}Xe, generated by spin exchange optical pumping (SEOP),[1] enabled its use in applications such as lung imaging and probing porous materials. The solubility of xenon in water is sufficient to make measurement of dissolved hyperpolarized ^{129}Xe signals easy, and the sensitivity of xenon's chemical shift to the local environment reports on interactions in the solution. Most interactions with xenon are weak and exchange among interaction sites is fast, so the shift reflects a population average over interacting sites. To enable sensing of a specific target we developed molecular sensors that combine a xenon binding cage, cryptophane-A,[2−5] with a target-binding element.[6−9]

Binding of the targeting element of the sensor to the target causes a small further shift of the encapsulated xenon, reporting on the interaction and, hence, the presence of the target. Although xenon exchange is slow enough to give a separate resonance, it is sufficiently fast that chemical exchange saturation transfer (CEST) effects can be large. We showed that hyperpolarized xenon CEST[10] (hyper-CEST) can be used for highly sensitive detection of targets into the picomolar concentration range[8] and can be used as contrast agents for xenon MRI to visualize the distribution of the target molecule in optically opaque samples. Sensors for specific ions, proteins, and nucleic acids have been developed,[11−13] and variants of cryptophane-A (binding constant 850 M^{-1}) and other compounds have been identified with even better exchange properties.[14]

The hyper-CEST detection method requires selective saturation of the cage-associated xenon peak, which means that it must be resolved from the bulk xenon peak. Even at moderately high fields, resolving the peaks is not a problem because the cryptophane-associated shift is about 120 ppm from the bulk dissolved xenon. Discriminating free and target-bound sensor is more challenging because binding-induced shifts are a few parts per million.[15] Since the magnetization from hyperpolarization is independent of field, we wanted to explore whether alternative sensors could be developed that would remove the hyper-CEST requirement. To this end, we prepared a new sensor for studies of binding induced xenon relaxation, M2B1 (Figure 1) that combines cryptophane for binding xenon, a targeting element, and a DOTA chelator to allow introduction of paramagnetic metals.

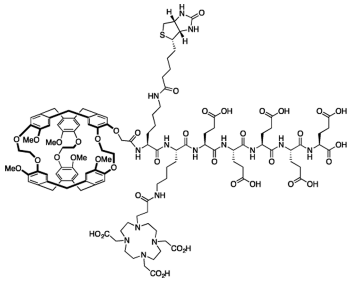

Figure 1. Relaxation sensor, M2B1, consists of a cryptophane cage modified with a DOTA for metal ion chelation, a biotin for avidin binding, and glutamate residues for solubilization. The designation, M2B1, refers to the placement of the metal-binding moiety at position 2 and biotin at position 1 of the peptide chain.

NMR relaxation rates are sensitive to the magnitude of magnetic interactions of the spins studied (e.g., dipole moments of other spins nearby and chemical shift anisotropy) and also their time dependence, arising from molecular tumbling in solution. We exploit the difference in tumbling correlation time between a free sensor and one that is bound to a high molecular weight target.[16−19] Relaxed xenon in the cage is exchanged into solution at a rate much higher than the relaxation rate of bulk xenon and, hence, affects the bulk xenon

Received: March 15, 2016
Published: July 29, 2016

DOI: 10.1021/jacs.6b02758
J. Am. Chem. Soc. 2016, 138, 9747−9750

relaxation as well. Detection of the target is achieved by determining the change in relaxation rates of the bulk xenon, a form of relaxometry.

Here we show that there are significant differences in the relaxation rate for xenon in solution with the sensor alone and xenon in solution with the sensor bound to a macromolecular target, like avidin. The changes are sufficiently large to allow use of relaxation rates to detect the association of the sensor with the target and, hence, the presence of the target in the sample. We have used detection of avidin as a model system, but this sensing principle can be extended to a wide variety of possible targets. The only requirement is that the target is sufficiently larger than the sensor (2 kDa) to alter the rotational correlation time.

Monoacid cryptophane-A cage was covalently attached to the N-terminus of a seven amino acid peptide chain (KKEEEEE) that was further derivatized with 1,4,7,10-tetraaza-cyclododecane-1,4,7,10-tetraacetic acid, DOTA, and biotin through the lysine amino groups (Figure 1). For binding studies with avidin, which is a tetramer with four biotin sites, the sensor was added to avidin in a 4:1 ratio. DOTA forms very stable complexes with most metals; in this work both metal-free and Gd^{3+}-bound forms were studied.

For all experiments, the sensors and controls were dissolved in 10 mM PBS (pH 7). Each sample was pressurized to 50 psi with a mixture of 2% natural isotopic abundance xenon gas, 10% nitrogen. and 88% helium gas mixture (natural abundance of ^{129}Xe is 26%). ^{129}Xe in this mixture was hyperpolarized using a home-built SEOP xenon polarizer and then bubbled into the sample at a flow rate of 0.4 standard L/min. Bubbling was stopped before acquisition to allow bubbles to dissipate. T_2 relaxation times of the bulk xenon resonance were measured with a standard CPMG pulse sequence. T_1 relaxation times of the bulk xenon resonance were measured by means of a single-shot decay signal using a Look-Locker pulse sequence.[20] This sequence minimizes the shot noise of each measurement and reduces the measurement time. Relaxation times for a solution containing stoichiometric amounts of sensor added to avidin were also measured. All data were collected on a 9.4 T Varian Inova NMR spectrometer at 293 K.

The relaxation of xenon in water is known to be very slow because fluctuations of the water around xenon are very rapid, consistent with the values we observed (see Table 1). The addition of M2B1 to the solution decreases the T_2. The broadening of bulk xenon due to exchange in and out of the cage is quite small (less than 1% of xenon is bound, and the exchange rate is ~20 s^{-1}), consistent with a modest decrease in relaxation time.[21] The addition of avidin alone to the xenon solution causes exchange broadening, but the process is near the fast exchange limit reflecting transient binding of the xenon. Similar weak binding and broadening of xenon has been seen for many proteins.[22] Adding biotin to a solution of avidin increased the T_2 of xenon because the biotin-binding pockets of the protein are no longer open to xenon. When M2B1 and avidin are both added to the solution, the biotin on the sensor binds to avidin, and the cryptophane cage is substantially immobilized. The sensor also interacts nonspecifically with avidin, which decreases the bulk T_2 of xenon.

To calculate the effects of bound state ^{129}Xe T_2 relaxation on the bulk ^{129}Xe, it is necessary to use the Carver Richards equation in its corrected form,[23] which treats the second-order exchange process and the effects of the Carr Purcell sequence. The analysis, discussed in the Supporting Information, shows that exchanged transferred T_2 relaxation can contribute significantly to the bulk xenon relaxation when the occupancy of the cage is significant and the cage bound T_2 relaxation is fast. The slowed tumbling of the cryptophane cage when bound to avidin results in faster relaxation of xenon in the cage giving a roughly 4-fold reduction in the bulk xenon T_2, shown in Table 1. The change in T_2 is apparent in the relaxation curves in Figure 2. The enhancement of relaxation upon association of the sensor with the target protein is the key element of this sensing approach. The difference in T_2 between the specific and nonspecific binding cases is about 14%. If the bulk T_2 is below the nonspecific binding T_2, then this indicates specific binding. The difference between specific and nonspecific binding can be increased by synthesizing a sensor with less amino acids.

Table 1. Relaxation Times of Xenon in Solutions of Sensor and Target Given as an Average and Standard Deviation of 10 Repetitions[a]

sample	T_2 (s)
1× PBS buffer	56.4 ± 0.6
5 μM M2B1	28.3 ± 0.4
1.5 μM avidin	11.2 ± 0.2
biotin-saturated 1.5 μM avidin	17.6 ± 0.2
5 μM M2B1 added to 1.5 μM biotin-saturated avidin	7.32 ± 0.08
5 μM M2B1 with 1.5 μM avidin	6.40 ± 0.03
5 μM M2B1 with 130 nM avidin	26.9 ± 0.6

[a]Each avidin tetramer binds four biotins and may also bind nonspecifically to the sensor.

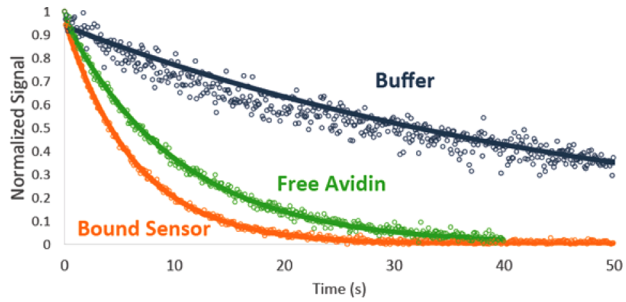

Figure 2. Plot of T_2 relaxation curves of xenon in buffer, xenon with avidin, and xenon with sensor bound to avidin showing dramatic enhancement of relaxation in the complex.

Improved xenon polarization or an isotopically enriched gas mixture would improve the signal-to-noise ratio and further improve the sensitivity of this technique. Higher molecular weight targets will give higher bound ^{129}Xe relaxation rates (proportional to the tumbling correlation time, roughly linear in molecular weight[24]) and, thus, also improve sensitivity.

In the design of M2B1 we included a tethered DOTA to bind a paramagnetic metal and potentially enhance the relaxation. Gd^{3+} is a very effective relaxation agent with seven unpaired electrons, and it binds very tightly to DOTA. The effect of the paramagnetic metal ion is discussed in the Supporting Information.

When the metal-chelated M2B1 is bound to the avidin, there is no improvement in xenon relaxivity relative to metal-free M2B1 (see Supporting Information).

A 1.5 μM solution of avidin (Figure 3A) has a relaxation time of 11 s. Adding biotin to the avidin solution increased the

DOI: 10.1021/jacs.6b02758
J. Am. Chem. Soc. 2016, 138, 9747−9750

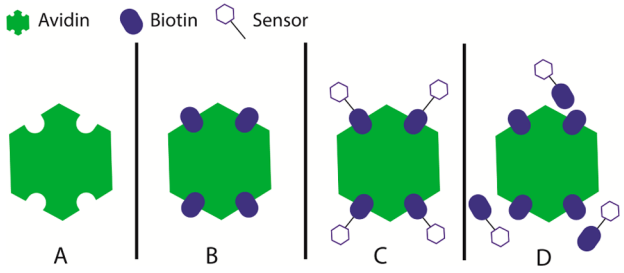

Figure 3. Tested relaxation environments for specific and nonspecific binding interactions with avidin: (A) nonspecific binding of xenon gas to avidin with nothing bound to it; (B) relaxation of xenon with biotin-bound avidin; (C) sensor bound to avidin with the assumption that by adding stoichiometric amounts there is minimal nonspecific binding; (D) nonspecific binding of the sensor to avidin bound to biotin.

relaxation time to 17.6 s (Figure 3B) suggesting that the biotin-binding pocket also binds and relaxes xenon. The sensor in a 5 μM concentration yields a 28 s relaxation time. Mixing the sensor with avidin (Figure 3C) reduces the xenon relaxation time to 6.4 s. The effectiveness of the sensor, however, also depends on nonspecific binding of the sensor to avidin, made possible by the hydrophilic peptide that solubilizes the cryptophane. The premixed biotin–avidin solution (Figure 3D) can no longer specifically bind the sensor, so adding it to the solution would, in the absence of any interaction, result in a relaxation time of 10.9 s calculated as the sum of relaxation rates of a solution containing only the sensor and a solution containing only avidin already bound to biotin. The measured relaxation time, however, was lower (7.3 s) confirming that there is a nonspecific sensor-avidin interaction. The sensor specifically bound to avidin relaxes at a rate approximately 40% faster, but strategies to reduce the nonspecific sensor–protein interaction would increase the overall contrast upon specific binding.

Due to the small amount of sensor necessary to observe relaxation contrast, shortening the solubilizing linker could significantly reduce nonspecific interactions while not reducing solubility to the point where it would no longer be effective. The solubility of the sensor is around 300 μM, so it should be possible to shorten its peptide chain while keeping it soluble. It is possible to imagine generating a solubilizing linker that acts as your targeting moiety for many systems or designing sensors that take advantage of the nonspecific binding.

Xenon NMR for sensing has exploited binding-induced shifts and saturation transfer for contrast generation, which both require resolution of chemically shifted peaks. Here we demonstrate that a sensor with a xenon-binding cage can act as a relaxation agent that responds to altered correlation times upon binding a macromolecular target. Even with a moderately sized protein target there is a dramatic enhancement of T_2 relaxation of the caged xenon, which is transferred to bulk xenon through exchange. This effect does not require chemical shift resolution. The relaxation effects will be increased for larger target molecules because T_2 relaxation scales with molecular weight.

■ ASSOCIATED CONTENT

Supporting Information

The Supporting Information is available free of charge on the ACS Publications website at DOI: 10.1021/jacs.6b02758.

General experimental procedures and materials; synthesis of avidin sensor; T_2 relaxation measurements; T_1 relaxation measurements; supplemental relaxation curves; paramagnetic metal ions; corrected Carver Richards equation (PDF)

■ AUTHOR INFORMATION

Corresponding Author

*pines@berkeley.edu

Notes

The authors declare no competing financial interest.

■ ACKNOWLEDGMENTS

This work was supported by the U.S. Department of Energy, Office of Science, Basic Energy Sciences, Materials Sciences and Engineering Division, under Contract No. DE-AC02-05CH11231 (to A.P.). C.C.S. acknowledges a National Science Foundation graduate fellowship under grant DGE-1106400. J.A.F. was supported by the Department of Defense (DoD) through the National Defense Science & Engineering Graduate (NDSEG) Fellowship Program. J.A.F. was supported by the Department of Defense through the National Defense Science and Engineering Graduate Fellowship

■ REFERENCES

(1) Goodson, B. M. *J. Magn. Reson.* **2002**, *155*, 157.
(2) Kunth, M.; Witte, C.; Schröder, L.; Wi, L. *NMR Biomed.* **2015**, *28*, 601.
(3) Witte, C.; Martos, V.; Rose, H. M.; Reinke, S.; Klippel, S.; Schröder, L.; Hackenberger, C. P. R. *Angew. Chem., Int. Ed.* **2015**, *54*, 2806.
(4) Khan, N. S.; Riggle, B. A.; Seward, G. K.; Bai, Y.; Dmochowski, I. J. *Bioconjugate Chem.* **2015**, *26*, 101.
(5) Riggle, B. A.; Wang, Y.; Dmochowski, I. J. *J. Am. Chem. Soc.* **2015**, *137*, 5542.
(6) Qing, K.; Ruppert, K.; Jiang, Y.; Mata, J. F.; Miller, G. W.; Shim, Y. M.; Wang, C.; Ruset, I. C.; Hersman, F. W.; Altes, T. A.; Mugler, J. P. *J. Magn. Reson. Imaging* **2014**, *39*, 346.
(7) Zamberlan, F.; Lesbats, C.; Rogers, N. J.; Krupa, J. L.; Pavlovskaya, G. E.; Thomas, N. R.; Faas, H. M.; Meersmann, T. *ChemPhysChem* **2015**, *16*, 2476.
(8) Stevens, T. K.; Palaniappan, K. K.; Ramirez, R. M.; Francis, M. B.; Wemmer, D. E.; Pines, A. *Magn. Reson. Med.* **2013**, *69*, 1245.
(9) Tassali, N.; Kotera, N.; Boulard, Y.; Rousseau, B.; Dubost, E.; Brotin, T.; Dutasta, J.; Berthault, P. *Anal. Chem.* **2014**, *86*, 1783.
(10) Schröder, L.; Lowery, T. J.; Hilty, C.; Wemmer, D. E.; Pines, A. *Science* **2006**, *314*, 446.
(11) Kunth, M.; Witte, C.; Hennig, A.; Schröder, L. *Chem. Sci.* **2015**, *6*, 6069.
(12) Meldrum, T.; Seim, K. L.; Bajaj, V. S.; Palaniappan, K. K.; Wu, W.; Francis, M. B.; Wemmer, D. E.; Pines, A. *J. Am. Chem. Soc.* **2010**, *132*, 5936.
(13) Roy, V.; Brotin, T.; Dutasta, J.-P.; Charles, M.-H.; Delair, T.; Mallet, F.; Huber, G.; Desvaux, H.; Boulard, Y.; Berthault, P. *ChemPhysChem* **2007**, *8*, 2082.
(14) Wang, Y.; Dmochowski, I. J. *Chem. Commun.* **2015**, *51*, 8982.
(15) Garimella, P. D.; Meldrum, T.; Witus, L. S.; Smith, M.; Bajaj, V. S.; Wemmer, D. E.; Francis, M. B.; Pines, A. *J. Am. Chem. Soc.* **2014**, *136*, 164.
(16) Lowery, T. J.; Garcia, S.; Chavez, L.; Ruiz, E. J.; Wu, T.; Brotin, T.; Dutasta, J.-P.; King, D. S.; Schultz, P. G.; Pines, A.; Wemmer, D. E. *ChemBioChem* **2006**, *7*, 65.
(17) Hall, L. D.; Evans, S. D.; Nott, K. P. *Magn. Reson. Imaging* **1998**, *16*, 485.
(18) Jaeger, F.; Bowe, S.; Van As, H.; Schaumann, G. E. *Eur. J. Soil Sci.* **2009**, *60*, 1052.

DOI: 10.1021/jacs.6b02758
J. Am. Chem. Soc. 2016, 138, 9747–9750

(19) Allsopp, K.; Wright, I.; Lastockin, D.; Mirotchnik, K.; Kantzas, A. *J. Can. Pet. Technol.* **2005**, *40*, 58.
(20) Look, D. C. *Rev. Sci. Instrum.* **1970**, *41*, 250.
(21) Spence, M. M.; Ruiz, E. J.; Rubin, S. M.; Lowery, T. J.; Winssinger, N.; Schultz, P. G.; Wemmer, D. E.; Pines, A. *J. Am. Chem. Soc.* **2004**, *126*, 15287.
(22) Rubin, S. M.; Spence, M. M.; Pines; Wemmer, D. E. *J. Magn. Reson.* **2001**, *152*, 79.
(23) Baldwin, A. J. *J. Magn. Reson.* **2014**, *244*, 114.
(24) Gore, J. C.; Anderson, A. W. *eMagRes.* **2013**, *1*, 67.

DOI: 10.1021/jacs.6b02758
J. Am. Chem. Soc. 2016, 138, 9747−9750